

Research Article

Effect of Hydrophilicity/Hydrophobicity of the Injector Wall on Atomization Performance

Xiaoyu Zhang ¹, Xiaolei Zhang ¹, Runze Duan ^{1,2} and Lujia Liu ³

¹School of Energy and Environmental Engineering, Hebei University of Technology, Tianjin 300401, China

²Hebei Key Laboratory of Thermal Science and Energy Clean Utilization, Tianjin 300401, China

³Institute of Fundamental Technological Research, Polish Academy of Sciences, Pawińskiego 5b, 02-106 Warsaw, Poland

Correspondence should be addressed to Runze Duan; duanrunze@hebut.edu.cn

Received 17 June 2022; Accepted 23 August 2022; Published 4 October 2022

Academic Editor: Yiheng Tong

Copyright © 2022 Xiaoyu Zhang et al. This is an open access article distributed under the Creative Commons Attribution License, which permits unrestricted use, distribution, and reproduction in any medium, provided the original work is properly cited.

Hydrophilicity/hydrophobicity is a common physical property of the material. Water droplets roll on lotus leaf, and a lot of dust and dirt on the surface of the lotus leaf will be taken away, playing a certain cleaning role. The hydrophobic surface has drag reduction effect that would produce slip on the hydrophobic wall. There are some studies on hydrophilicity/hydrophobicity in channels, most of which focus on the effect of surface drag reduction and heat transfer on microchannels. However, few people pay attention to the effect of the hydrophilicity/hydrophobicity of the injector inner wall on the atomization performance. In this paper, three groups of the open-end swirl injector with different tangential channels were designed to study the effect of hydrophilicity/hydrophobicity on atomization performance. The hydrophobic coating was prepared and used on the inner wall of the injector, and the atomization experimental system was built. In the experiment, the liquid film thickness was measured using the conductance method. Details of the liquid film breakup and spray development were recorded with a high-speed camera. The average droplet diameter was measured by the Malvern particle size analyzer. The atomization performance of injectors with different tangential channels on the hydrophilicity/hydrophobicity was compared, and the effect of the velocity profile on the jet stability is discussed.

1. Introduction

The hydrophilicity/hydrophobicity of the solid wall reflects the different characteristics of the liquid and the solid contact. The liquid will fit better on the hydrophilic wall with the solid wall but the liquid will slip on the hydrophobic wall. When the liquid droplet rolls on the solid wall, it will remove stains on the solid wall, which make that hydrophobic wall has self-cleaning property. The hydrophobic surface has drag reduction effect, which causes a slip flow at the solid-liquid interface, and the velocity gradient at the interface is reduced, so that the laminar flow state of the attachment surface is kept more stable and the shear force at the solid-liquid interface is reduced. Some chemical reactions on the substrate will make the substrate hydrophobic [1–4], thus achieving the purpose of the

artificially preparing a hydrophobic coating. Yamashita et al. [5] firstly prepared the superhydrophobic surfaces and carried out the experimental research. They sprayed a layer of the photocatalyst with TiO_2 as the main material on the surface of the polytetrafluoroethylene (ordinary hydrophobic material) and finally obtained a superhydrophobic surface. The surface has the “automatic cleaning” feature, and the liquid can roll freely on the surface and carry away stains. Cremaldi and Bhushan [6] used a chemical etching method to create a micro-nanostructure on the surface of the stainless steel, which hydrophobizes the surface of the stainless steel. Vilaio and Yague [7] conducted a hydrophobic surface preparation experiment for the copper sheets. This experiment used a chemical etching method to etch a micron-scale roughness on the surface of the copper, and the coating can effectively

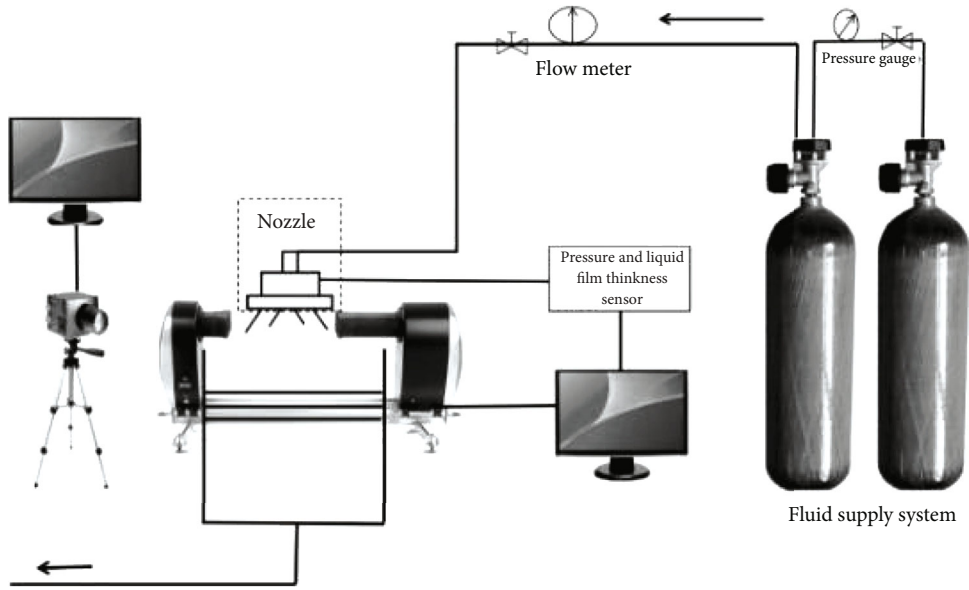


FIGURE 1: Experimental system.

TABLE 1: Properties of experimental equipment.

Equipment	Measurement range	Precision
Flow meter	0–0.4 m ³ /h	±1%
Pressure gauge	0–1 MPa	0.5%

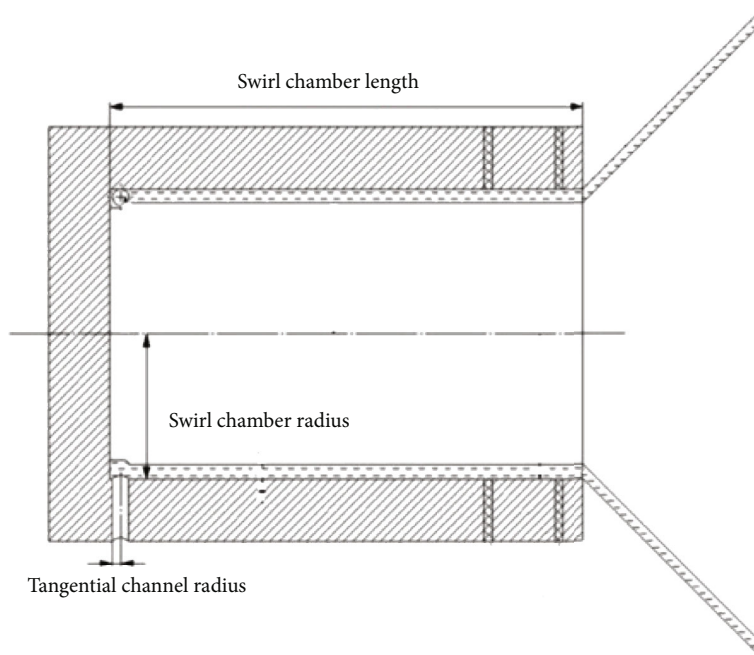


FIGURE 2: Open-end swirl injector.

protect the copper substrate and the display excellent corrosion resistance. Nine et al. [8] developed a new type of the composite hydrophobic coating, which was mainly prepared by mixing polydimethylsiloxane (PDMS), diatomaceous earth, and reduced graphene oxide (rGO). Sungnam et al. [9] found

that the surface of the conventional channel can exhibit an obvious flow drag reduction effect after $Re < 200000$ on the surface after the superhydrophobic treatment. Using the drag reduction characteristics of the superhydrophobic surfaces, Rosengarten et al. [10] studied the effects of the contact angle

TABLE 2: Injector structure parameters.

Number	Tangential channel radius (mm)	Swirl chamber radius (mm)	Swirl chamber length (mm)
Injector 1	1.35	8.00	43.5
Injector 2	1.10	8.00	43.5
Injector 3	0.90	8.00	43.5

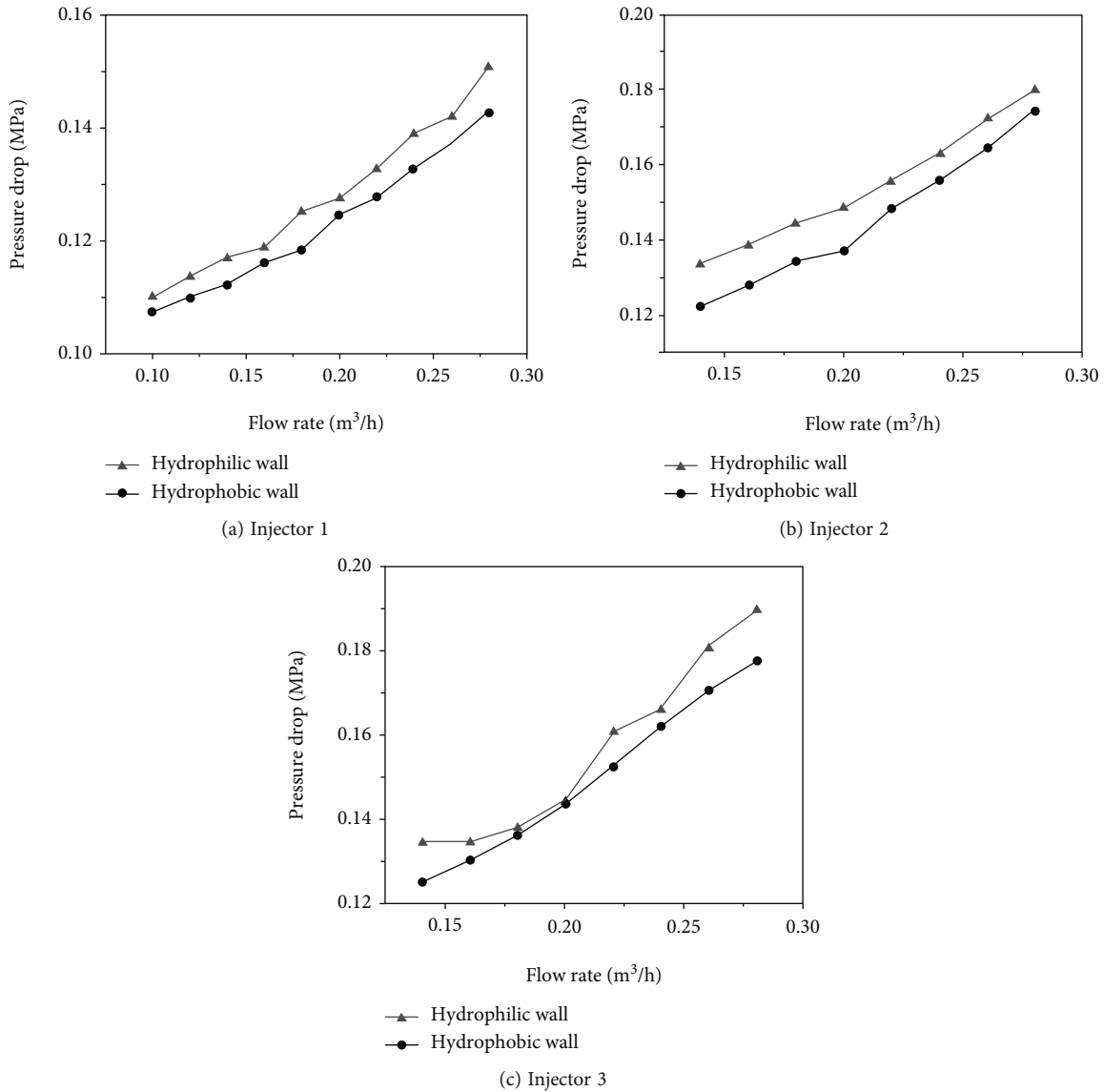


FIGURE 3: Effect of the flow rate on the injector pressure drop in different injectors.

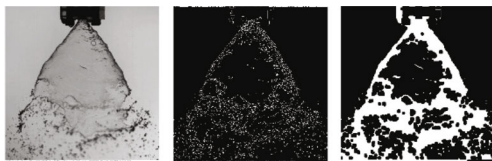


FIGURE 4: Extraction of the spray cone angle.

on the inner wall of the microchannels on the single relative flow heat transfer and water flowing. Studying the performance of the hydrophobic surfaces requires consideration of the effect of the surface roughness on the hydrophobic properties with two different models, the Wenzel model [11] and the Cassie model [12] which show different contact states between the droplet and the solid surface.

Many designs of the rocket engines have high requirements on the drag reduction performance of the material surface

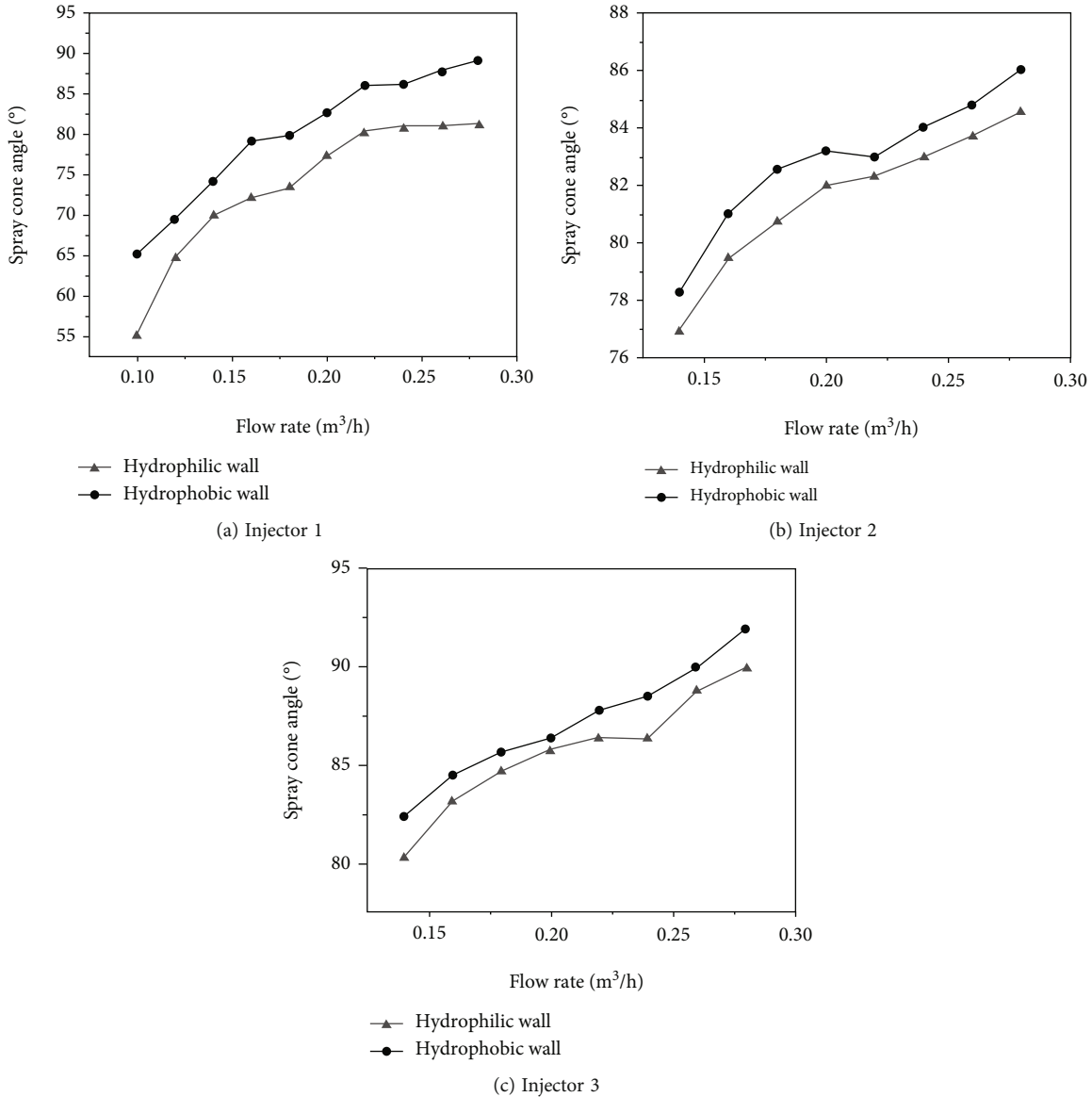


FIGURE 5: Effect of the flow rate on the injector spray cone angle in different injectors.

[13–15], but the application of the hydrophobic surfaces on the engine has not been carried out. Many studies focus on the liquid film breaking mechanism and the atomization characteristics of the normal surface, but the effect of the hydrophobic surfaces on the atomization has not received much attention. In this paper, three groups of the open-end swirl injectors with different tangential channels were designed to study the effect of the hydrophilicity/hydrophobicity on the atomization performance.

2. Experimental System

In this paper, a superhydrophobic nanoclear coating solution [16, 17] is used as a raw material for the hydrophobic coating. Inorganic nanoparticles, dispersant, crosslinking agent, etc. are sequentially added in an organic solvent and ultrasonically dispersed to obtain the hydrophobic coating. Hydrophobic coating

is prepared by immersing the injector in a uniformly mixed coating solution. The contact angle reflects the hydrophobic properties of the hydrophobic wall, and the larger the surface contact angle is, the better the hydrophobic properties are. The surface contact angle of the injector treated with the above hydrophobic solution was 117.76° , which was considered to meet the hydrophobic requirements.

The experimental system is shown in Figure 1. In this experiment, the flow rate was adjusted by the valve near the flow meter and pressure drop was measured by the pressure gauge, which was the pressure difference between the injector inlet and outlet. The picture of the spray field during the atomization process was taken by the high-speed camera and saved to the computer. At the same time, the data was collected by the data acquisition system. The data acquisition system includes the pressure sensor, the voltage signal, and the liquid film thickness sensor connected to the injector. The average

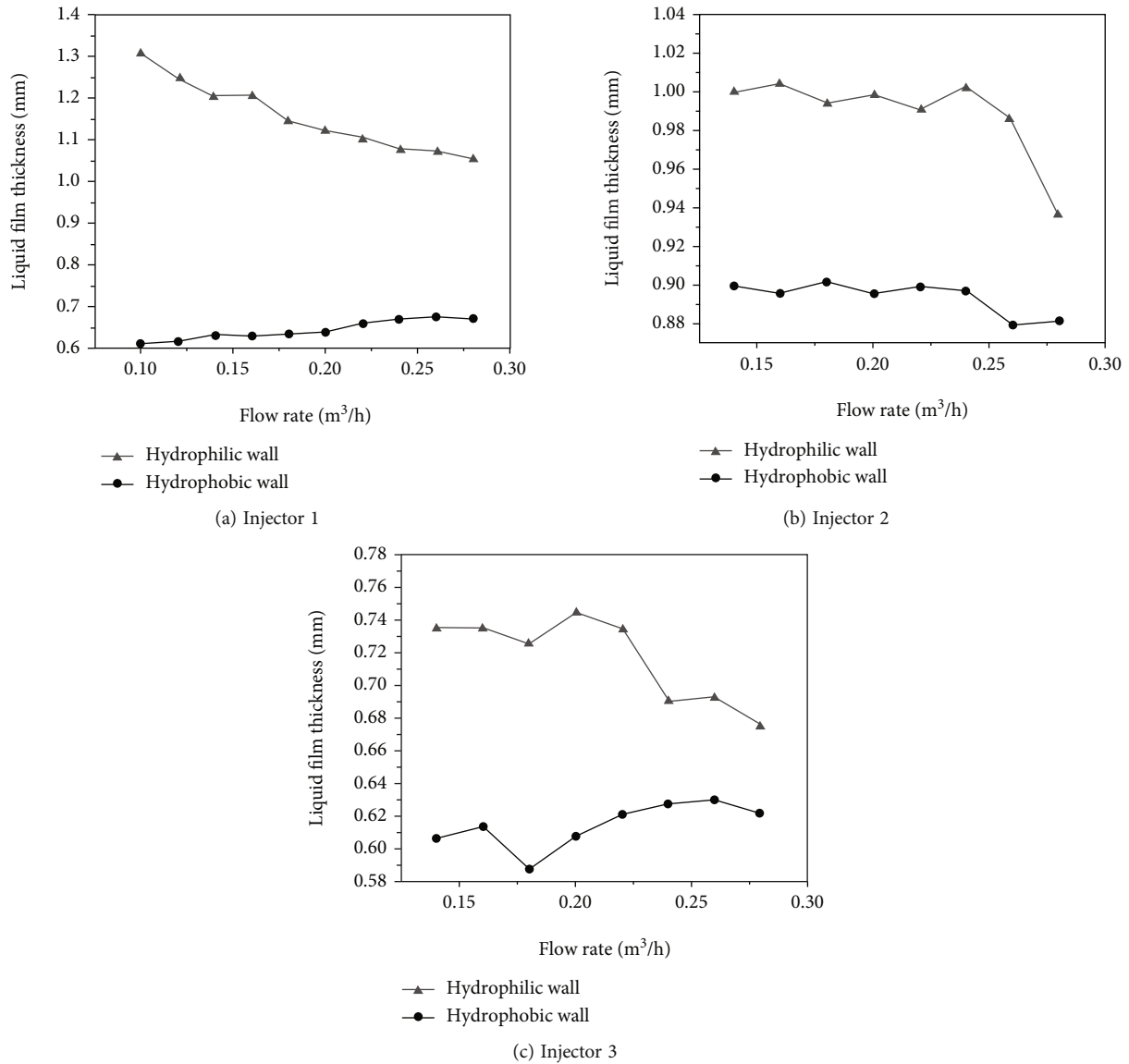


FIGURE 6: Effect of the flow rate on liquid film thickness in different injectors.

droplet diameter was measured by the Malvern particle size analyzer. The parameters of the flowmeter and the pressure gauge are shown in Table 1. When the flow rate reached 0.3 m³/h in the experiment, the hydrophilic/hydrophobic wall pressure signal began to converge and the hydrophobic coating was considered to be detached, so the maximum flow rate of the hydrophobic coating is 0.3 m³/h. The flow range in the paper is 0.1 m³/h–0.3 m³/h.

Figure 2 shows the test injector that is an open-end swirl injector with three different tangential channels, and the geometric parameters are shown in Table 2. The swirl intensity of the injectors was changed by the variety of the tangential channel radius.

3. Results and Discussion

3.1. Effect of the Flow Rate on the Injector Pressure Drop.

Figure 3 shows the change in injector pressure drop for dif-

ferent tangential channels. It can be seen that the pressure drop inside the injector increases with the increase of the flow rate of the liquid. While comparing the hydrophobic the pressure drop with the hydrophilic pressure drop, it can be found that the pressure drop inside the hydrophobic injector will be smaller than that of the hydrophilic injector under the same conditions. The hydrophobic coating can cause the fluid flowing through the inner wall surface of the injector to slip and reduce the resistance, thereby decreasing the pressure drop inside the injector. The pressure drop increases with the decrease of the tangential channel radius of the injector for three different injectors in Figure 3.

3.2. Effect of the Flow Rate on the Injector Spray Cone Angle.

The atomization process was photographed with a high-speed camera to obtain a photograph of the spray field, as shown in Figure 4. The shooting frame rate is 2000 fps,

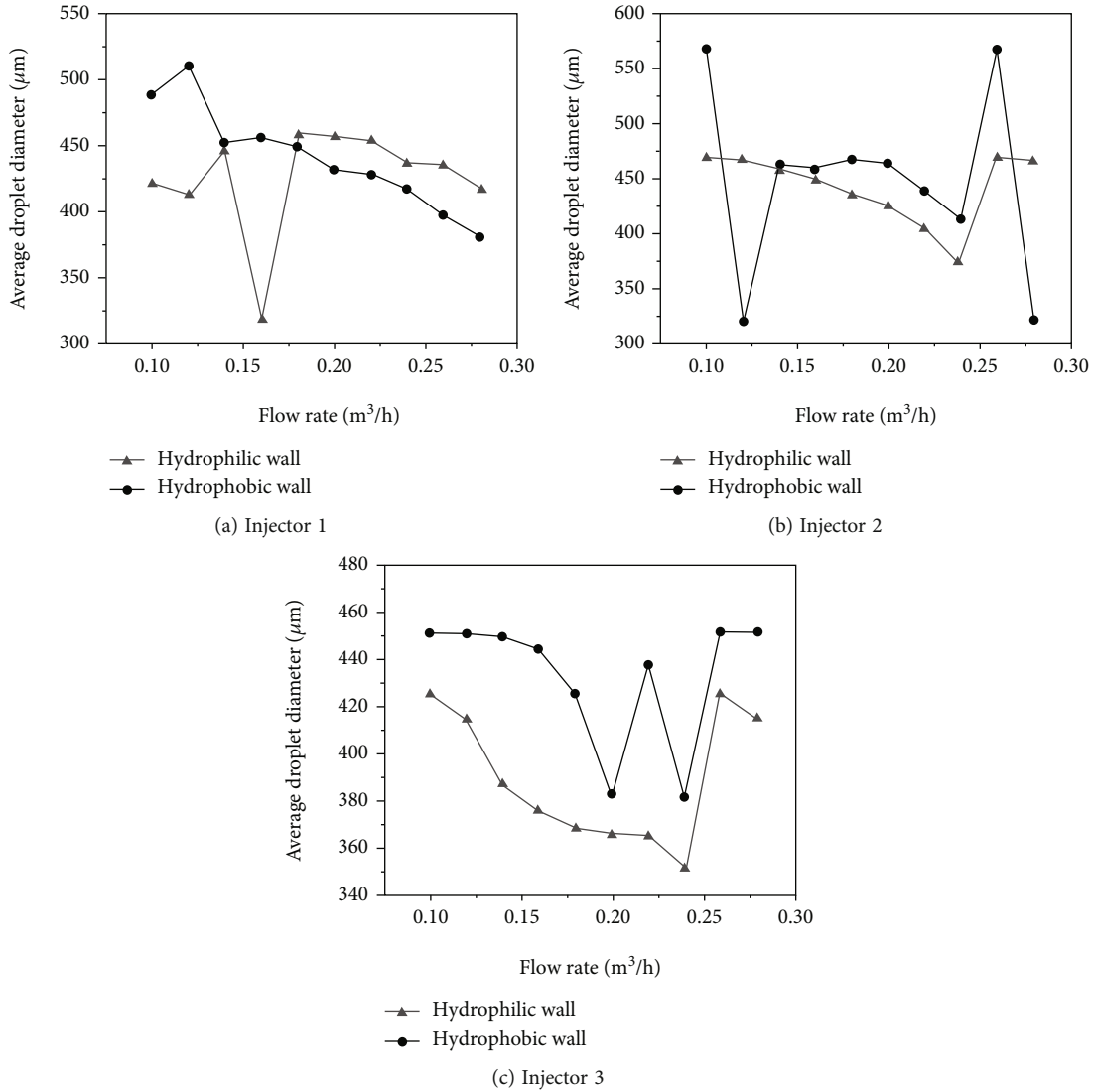


FIGURE 7: Effect of the flow rate on the average droplet diameter in different injectors.

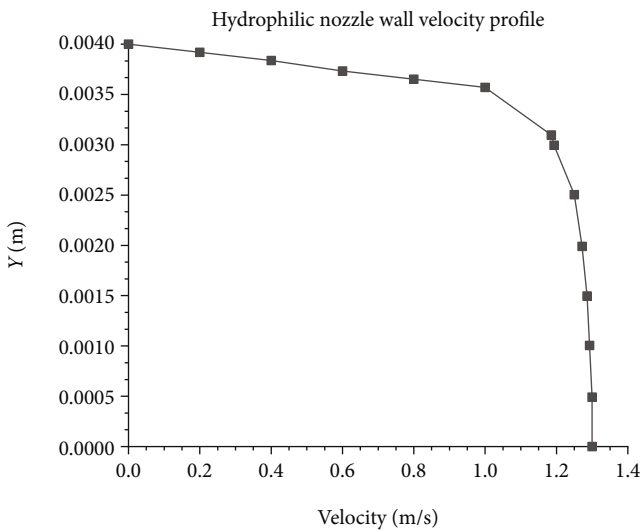


FIGURE 8: Hydrophilic wall velocity profile.

and the minimum exposure time is 20 μs . The image in the stable interval during the atomization process was obtained. The obtained image was binarized to obtain a spray angle boundary, thereby obtaining a spray cone angle. The effect of the flow rate on the injector spray cone angle for different tangential channels is shown in Figure 5. It shows that the spray cone angle of the hydrophilic injector and the hydrophobic injector increase with the increase of the flow rate, and the spray cone angle of the hydrophobic injector comparing the angle with the hydrophilic injector, it can be found that the spray cone angle of the hydrophobic injector becomes larger than that of the hydrophilic injector as wall surface slips.

3.3. *Effect of the Flow Rate on Liquid Film Thickness.* The conductance measurement method was used to determine the thickness of the liquid film [18–21]. The effect of flow rate on liquid film thickness at different flow rates was shown in Figure 6. It can be seen that the liquid film thickness of three injectors decreases with the increase of the flow rate. The liquid film thickness of the hydrophobic injector is

smaller than that of the hydrophilic injector under the same working condition as the hydrophobic inner wall surface reduces the velocity loss of the fluid.

3.4. Effect of the Flow Rate on the Average Droplet Diameter. The Malvern particle sizer is used to measure the average diameter of the droplets during the atomization, which can measure particles with a diameter in the range of 0–900 μm . The change in the diameter of the droplet determines whether the hydrophobic coating will have an effect on atomization. The effect of the flow rate on the average droplet diameter was investigated in Figure 7. By comparing the experimental results of three injectors, it can be found that the average droplet diameter of the hydrophobic injector is larger than that of the hydrophilic injector in the range of 0.1 m^3/h –0.18 m^3/h in injector 1 (the tangential channel diameter is 2.7 mm), but in the range of 0.18 m^3/h –0.28 m^3/h , the average diameter of the droplets of the hydrophobic injector is smaller than that of the hydrophilic injector; injector 2 (the tangential channel diameter is 2.2 mm) and injector 3 (the tangential channel diameter is 1.8 mm) can be seen that the droplet diameter of the hydrophobic injector is substantially larger than that of the hydrophilic injector. It is found that the average diameter of the droplets decreases with the increase of the flow rate, indicating that the increase of the flow rate reduces the average diameter of the droplet and increases the total surface area of the droplet.

3.5. Velocity Profile of the Liquid Film on the Hydrophilic Wall. The velocity profile of the injector wall affects the stability of the jet [22], [23]. The difference of the velocity profile of the hydrophilic walls was investigated by numerical simulation in Figure 8. The velocity profile of the hydrophilic wall is similar to the parabolic jet velocity profiles as the jet velocity of the hydrophobic wall is very gentle. Flowing with a fully developed parabolic velocity profile, the kinetic energy of the fluid is exactly twice what it would be if the fluid was ideal (plug flow) and flowing at the same average velocity. The velocity profile of the hydrophobic wall surface will make the jet more stable than that of the hydrophilic wall surface. As the result, for the average diameter of the droplets, the hydrophobic wall has different effects on the atomization performance in different flow ranges.

4. Conclusions

In this paper, the atomization experiments of the hydrophilic/hydrophobic injectors were carried out using three different tangential channel centrifugal injectors. The following can be found:

- (1) The injector pressure drop after the hydrophobic treatment is decreased, the spray cone angle is increased, and the liquid film thickness is decreased
- (2) The average diameter of the droplets has different changes at different flow rates
- (3) The effect of the velocity profile on jet stability is discussed. The velocity profile of the hydrophobic wall

surface will make the jet more stable than that of the hydrophilic wall surface

Data Availability

The data that support the findings of this study are available from the corresponding author upon reasonable request.

Conflicts of Interest

The authors declare that they have no conflicts of interest.

Acknowledgments

This research was supported by the National Natural Science Foundation of China (Support no. 12042211), Natural Science Foundation of Hebei (nos. A2022202010 and E2019202460), Tianjin Science and Technology Program (nos. 22YDTPJC00200 and 19YFZCSF00850), Key Research Program Projects of Hebei Province (no. 19274502D), and Industrial Technology Research of Hebei University of Technology (no. ZBYJY201902) which are gratefully acknowledged.

References

- [1] M. Drouin, J. L. Arenas, and J. F. Paquin, "Incorporating a monofluoroalkene into the backbones of short peptides: evaluating the impact on local hydrophobicity," *ChemBioChem*, vol. 20, no. 14, pp. 1817–1826, 2019.
- [2] A. V. Rao, M. M. Kulkarni, and S. D. Bhagat, "Transport of liquids using superhydrophobic aerogels," *Journal of Colloid and Interface Science*, vol. 285, no. 1, pp. 413–418, 2005.
- [3] H. M. Shang, Y. Wang, S. J. Limmer, T. P. Chou, K. Takahashi, and G. Z. Cao, "Optically transparent superhydrophobic silica-based films," *Thin Solid Films*, vol. 472, no. 1–2, pp. 37–43, 2005.
- [4] M. Karthika, H. Chi, T. D. Li, H. J. Wang, and S. Thomas, "Super-hydrophobic graphene oxide-azobenzene hybrids for improved hydrophobicity of polyurethane," *Composites Part B: Engineering*, vol. 173, article 106978, 2019.
- [5] H. Yamashita, H. Nakao, M. Takeuchi, Y. Nakatani, and M. Anpo, "Coating of TiO_2 photocatalysts on superhydrophobic porous teflon membrane by an ion assisted deposition method and their self-cleaning performance," *Nuclear Instruments and Methods in Physics Research Section B: Beam Interactions with Materials and Atoms*, vol. 206, pp. 898–901, 2003.
- [6] J. Cremaldi and B. Bhushan, "Fabrication of bioinspired, self-cleaning superliquiphilic/phobic stainless steel using different pathways," *Journal of Colloid and Interface Science*, vol. 518, pp. 284–297, 2018.
- [7] I. Vilaio and J. L. Yague, "Superhydrophobic copper surfaces with anticorrosion properties fabricated by solventless CVD methods," *ACS Applied Materials & Interfaces*, vol. 9, no. 1, pp. 1057–1065, 2017.
- [8] M. J. Nine, M. A. Cole, L. Johnson, D. N. H. Tran, and D. Losic, "Robust superhydrophobic graphene-based composite coatings with self-cleaning and corrosion barrier properties," *ACS Applied Materials & Interfaces*, vol. 7, no. 51, pp. 28482–28493, 2015.

- [9] L. Sungnam, C. N. Dang, and K. Dongseob, "Experimental drag reduction study of super-hydrophobic surface with dual-scale structures," *Applied Surface Science*, vol. 286, pp. 206–211, 2013.
- [10] G. Rosengarten, J. Cooper-White, and G. Metcalfe, "Experimental and analytical study of the effect of contact angle on liquid convective heat transfer in microchannels," *Heat and Mass Transfer*, vol. 49, no. 21-22, pp. 4161–4170, 2006.
- [11] M. Aevizeh, A. Darvizehv, and H. Rajabi, "Free vibration analysis of dragonfly wings using finite element method," *The International Journal of Multiphysics*, vol. 3, no. 1, pp. 101–110, 2009.
- [12] A. Khila, E. Abouheif, and L. Rowe, "Evolution of a novel appendage ground plan in water striders is driven by changes in the hox gene *Ultrabithorax*," *PLoS Genetics*, vol. 5, no. 7, article e1000583, 2009.
- [13] P. H. Li, L. J. Yang, and Q. F. Fu, "Effect of surface contact angle on the wall impingement of a power-law liquid jet," *Physics of Fluids*, vol. 33, no. 4, article 043105, 2021.
- [14] A. A. Ibrahim and M. A. Jog, "Nonlinear instability of an annular liquid sheet exposed to gas flow," *International Journal of Multiphase Flow*, vol. 34, no. 7, pp. 647–664, 2008.
- [15] L. H. Liu, Q. F. Fu, and L. J. Yang, "Linear stability analysis of liquid jet exposed to subsonic crossflow with heat and mass transfer," *Physics of Fluids*, vol. 33, no. 3, article 034111, 2021.
- [16] Q. F. Fu, F. Ge, W. D. Wang, and L. J. Yang, "Spray characteristics of gel propellants in an open-end swirl injector," *Fuel*, vol. 254, article 115555, 2019.
- [17] K. Y. Law, "Definitions for hydrophilicity, hydrophobicity, and superhydrophobicity: getting the basics right," *Journal of Physical Chemistry Letters*, vol. 5, no. 4, pp. 686–688, 2014.
- [18] C. J. Choi and H. K. Cho, "Investigation on emergency core coolant bypass with local measurement of liquid film thickness using electrical conductance sensor fabricated on flexible printed circuit board," *International Journal of Heat and Mass Transfer*, vol. 139, pp. 130–143, 2019.
- [19] Q. F. Fu, L. J. Yang, Y. Y. Qu, and B. Gu, "Geometrical effects on the fluid dynamics of an open-end swirl injector," *Journal Propulsion and Power*, vol. 27, no. 5, pp. 929–936, 2011.
- [20] Q. F. Fu, Y. X. Zhang, C. J. Mo, and L. J. Yang, "Molecular dynamics study on the mechanism of nanoscale jet instability reaching supercritical conditions," *Applied Sciences*, vol. 8, no. 10, p. 1714, 2018.
- [21] Q. F. Fu, Z. X. Fang, Y. X. Zhang, and L. J. Yang, "Molecular dynamics simulation of a jet in a binary system at supercritical environment," *Molecules*, vol. 24, p. 31, 2019.
- [22] A. Lozano, F. Barreras, G. Hauke, and C. Dopazo, "Longitudinal instabilities in an air-blasted liquid sheet," *Journal of Fluid Mechanics*, vol. 437, pp. 143–173, 2001.
- [23] E. A. Ibrahim, "Instability of a liquid sheet of parabolic velocity profile," *Physics of Fluids*, vol. 10, no. 4, pp. 1034–1036, 1998.